

## Visual experience shapes the neural networks remapping touch into external space

Abbreviated title: role of vision for tactile localization

Virginie Crollen<sup>1\*</sup>, Latifa Lazzouni<sup>3</sup>, Mohamed Rezk<sup>2</sup>, Antoine Bellemare<sup>3</sup>, Franco Lepore<sup>3</sup>,  
and Olivier Collignon<sup>1,2,3\*</sup>

*1. Centre for Mind/Brain Science, University of Trento, 38123 Mattarello TN, Italy; 2. Institute of Psychology (IPSY) and Institute of Neuroscience (IoNS), Université Catholique de Louvain, 1348 Louvain-la-Neuve, Belgium; 3. Centre de Recherche en Neuropsychologie et Cognition (CERNEC), Université de Montréal, H2V 2S9 Montreal, Canada.*

**\* Corresponding authors:** Virginie Crollen, CIMeC – Center for Mind/Brain Sciences, University of Trento, via delle Regole 101, 38123 Mattarello (TN), Italy. Email: [virginie.crollen@unitn.it](mailto:virginie.crollen@unitn.it); Olivier Collignon, Institut de Recherche en Sciences Psychologiques (IPSY), Centre de Neuroscience Système et Cognition, Université Catholique de Louvain, Place Cardinal Mercier 10, 1348 Louvain-la-Neuve, Belgium. Email: [olivier.collignon@uclouvain.be](mailto:olivier.collignon@uclouvain.be).

Number of pages: 20

Number of figures: 1

Number of tables: 2

Words count (abstract): 153

Words count (introduction): 404

Words count (discussion): 1169

### Acknowledgments

The authors are grateful to Giulia Dormal for her help in implementing the experimental design. This research and the authors were supported by the Canada Research Chair Program (FL), the Canadian Institutes of Health Research (FL), the Belgian National Funds for Scientific Research (VC), a WBI.World grant (VC), the European Union's Horizon 2020 research and innovation programme under the Marie Skłodowska-Curie grant agreement No 700057 (VC) and the 'MADVIS' European Research Council starting grant (OC; ERC-StG 337573). O.C. is a research associate at the Belgian National Fund for Scientific Research. The authors declare no competing financial interest

1 **Abstract**

2 Localizing touch relies on the activation of skin-based and externally defined spatial frames of  
3 references. Psychophysical studies have demonstrated that early visual deprivation prevents the  
4 automatic remapping of touch into external space. We used fMRI to characterize how visual  
5 experience impacts on the brain circuits dedicated to the spatial processing of touch. Sighted and  
6 congenitally blind humans (male and female) performed a tactile temporal order judgment (TOJ)  
7 task, either with the hands uncrossed or crossed over the body midline. Behavioral data confirmed  
8 that crossing the hands has a detrimental effect on TOJ judgments in sighted but not in blind.  
9 Crucially, the crossed hand posture elicited more activity in a fronto-parietal network in the sighted  
10 group only. Psychophysiological interaction analysis revealed that the congenitally blind showed  
11 enhanced functional connectivity between parietal and frontal regions in the crossed versus  
12 uncrossed hand postures. Our results demonstrate that visual experience scaffolds the neural  
13 implementation of touch perception.

14

15

16 **Significance statement**

17 Although we seamlessly localize tactile events in our daily life, it is not a trivial operation because  
18 the hands move constantly within the peripersonal space. To process touch correctly, the brain has  
19 therefore to take the current position of the limbs into account and remap them to their location in  
20 the external world. In sighted, parietal and premotor areas support this process. However, while  
21 visual experience has been suggested to support the implementation of the automatic external  
22 remapping of touch, no studies so far have investigated how early visual deprivation alters the brain  
23 network supporting touch localization. Examining this question is therefore crucial to conclusively  
24 determine the intrinsic role vision plays in scaffolding the neural implementation of touch  
25 perception.

26

## 27 Introduction

28           Quickly and accurately localizing touch in space is crucial for efficient action planning toward  
29 an external stimulus making contact with the body. Although we seamlessly do it in daily life, it is  
30 not a trivial operation because the hands move constantly within the peripersonal space as different  
31 postures are adopted. Therefore, the brain must transform tactile coordinates from an initial skin-  
32 based representation to a representation that is defined by coordinates in external space  
33 (Yamamoto and Kitazawa, 2001; Shore et al., 2002; Azañón and Soto-Faraco, 2008; Azañón et al.,  
34 2010a, 2015). For example, when sighted individuals have to judge which of their two hands receive  
35 a tactile stimulation first (Temporal Order Judgment task – TOJ), they do much more errors when  
36 their hands are crossed over the body midline compared to when the hands are uncrossed  
37 (Yamamoto and Kitazawa, 2001; Shore et al., 2002; Heed and Azañón, 2014). This crossed-hands  
38 deficit has been attributed to the misalignment of anatomical and external frames of reference  
39 (Yamamoto and Kitazawa, 2001; Shore et al., 2002). Because the task requirements have nothing  
40 spatial (in theory, the task could be solved by using somatotopic coordinates only), this crossing-  
41 hand effect compellingly illustrates how the external remapping of touch is automatic in sighted  
42 people (Heed and Azañón, 2014). Specific brain networks including parietal and premotor areas  
43 have been demonstrated to support this automatic remapping of touch into an external spatial  
44 coordinate system (Lloyd et al., 2003; Matsumoto et al., 2004; Azañón et al., 2010a; Takahashi et al.,  
45 2013; Wada et al., 2012).

46           Congenitally blind people, in contrast, do not show any crossing-hand deficit when involved  
47 in a tactile TOJ task (Röder et al., 2004; Crollen et al., 2017). This suggests that the default  
48 remapping of passive touch into external spatial coordinates is acquired during development as a  
49 consequence of visual experience. Does the absence of visual experience also alter the neural  
50 network typically recruited when people experience a conflict between skin-based and external  
51 spatial coordinates of touch? Investigating how congenital blindness reorganizes the brain network  
52 supporting touch localization is crucial to conclusively determine the intrinsic role vision plays in

53 scaffolding the neural implementation of the perception of touch location. In order to address this  
54 question, we used functional Magnetic Resonance Imaging (fMRI) to characterize the brain activity  
55 of congenitally blind individuals and sighted controls performing a tactile TOJ task with either their  
56 hands uncrossed or with the hands crossed over the body midline.

## 57 **Method**

### 58 ***Participants***

59 Eleven sighted controls (SC) [four females, age range 22-64 y, (mean  $\pm$  SD, 46  $\pm$  14 y)] and 8  
60 congenitally blinds (CB) participants [2 females, age range 24-63 y, (mean  $\pm$  SD, 47  $\pm$  13 y)] took part  
61 in the study (see Table 1 for a detailed description of the CB participants). The mean age of the SC  
62 and CB groups did not statistically differ ( $t(17) = 0.11, p = .92$ ). At the time of testing, the participants  
63 in the blind group were totally blind or had only rudimentary sensitivity for brightness differences  
64 and no patterned vision. In all cases, blindness was attributed to peripheral deficits with no  
65 additional neurological problems. Procedures were approved by the Research Ethics Boards of the  
66 University of Montreal. Experiments were undertaken with the understanding and written consent  
67 of each participant. Both groups of participants were blindfolded when performing the task.

68 **Table 1. Characteristics of the blind participants**

69

<i>Participants</i>	<i>Gender</i>	<i>Age</i>	<i>Handedness</i>	<i>Onset</i>	<i>Cause of blindness</i>
CB1	F	61	A	o	Retinopathy of prematurity
CB2	M	63	R	o	Congenital cataracts + optic nerve hypoplasia
CB3	F	32	A	o	Retinopathy of prematurity
CB4	M	56	R	o	Electrical burn of optic nerve bilaterally
CB5	M	24	R	o	Glaucoma and microphthalmia
CB6	M	52	A	o	Thalidomide
CB7	M	45	R	o	Retinopathy of prematurity

CB8

M

45 R

o

Leber's congenital amaurosis

---

70 Note. M = male; F = female; R = right-handed; A = ambidextrous.

### 71 ***Task and general experimental design***

72 In this task, two successive tactile stimuli were presented for 50 ms to the left and right  
73 middle fingers at 6 different stimulus onset asynchronies (SOAs): -120, -90, -60, 60, 90, 120.  
74 Negative values indicated that the first stimulus was presented to the participant's left hand;  
75 positive values indicated that the first stimulus was presented to the participant's right hand. Tactile  
76 stimuli were delivered using a pneumatic tactile stimulator (Institute for Biomagnetism and  
77 Biosignal Analysis, University of Muenster, Germany). A plastic membrane (1 cm in diameter) was  
78 attached to the distal phalanges of the left and right middle fingers and was inflated by a pulse of air  
79 pressure delivered through a rigid plastic tube. Participants had to press a response button placed  
80 below the index finger of the hand that they perceived to have been stimulated first. They had 3550  
81 ms to respond otherwise the trial was terminated. Participants were asked to perform the task  
82 either with their hands in a parallel posture (i.e., uncrossed posture) or with their arms crossed over  
83 the body midline. Stimuli were delivered and responses were recorded using Presentation software  
84 (Neurobehavioral Systems Inc.) running on a Dell XPS computer using a Windows 7 operating  
85 system.

86 Participants were scanned in 2 fMRI sessions using a block design. One run consisted of 16  
87 successive blocks (22 s duration each) separated by rest periods ranging from 11 to 14 s (median 12.5  
88 s), during which participants had to perform the TOJ judgments either with the hands uncrossed or  
89 with the hands crossed. The starting run (uncrossed or crossed) was counterbalanced across  
90 participants. Each block, either uncrossed or crossed, consisted of 6 successive pairs of stimulations  
91 (each SOA was randomly presented once in each block).

92 Before the fMRI acquisition, all participants underwent a training session in a mock scanner,  
93 with recorded scanner noise played in the bore of the stimulator to familiarize them with the fMRI  
94 environment and to ensure that the participants understood the task.

## 95 Behavioral data analyses

96 The mean percentages of “right hand first” responses were calculated for each participant,  
97 SOA and posture. These raw proportions were transformed into their standardized z-score  
98 equivalents and then used to calculate the best-fitting linear regression lines of each participant  
99 (Shore et al., 2002).

100 The just noticeable difference (JND; the smallest interval needed to reliably indicate  
101 temporal order) was secondly calculated from the mean slope data by subtracting the SOA needed  
102 to achieve 75% performance from the one needed to achieve 25% performance and dividing by 2  
103 (Shore et al., 2002). This value was calculated for the entire group. It could not be determined  
104 independently for all observers because several sighted people obtained a slightly negative slope  
105 value for the crossed posture (Shore et al., 2002). This indicated that some participants responded  
106 with the opposite hand as the one that has been stimulated first (Yamamoto and Kitazawa, 2001).

## 107 fMRI data acquisition and analyses

108 **Acquisition.** Functional MRI-series were acquired using a 3-T TRIO TIM system (Siemens, Erlangen,  
109 Germany), equipped with a 12-channel head coil. Multislice T<sub>2</sub>\*-weighted fMRI images were  
110 obtained with a gradient echo-planar sequence using axial slice orientation (TR = 2200 ms, TE =  
111 30 ms, FA = 90°, 35 transverse slices, 3.2 mm slice thickness, 0.8 mm inter-slice gap, FoV =  
112 192×192 mm<sup>2</sup>, matrix size = 64×64×35, voxel size = 3×3×3.2 mm<sup>3</sup>). Slices were sequentially acquired  
113 along the z-axis in feet-to-head direction. The 4 initial scans were discarded to allow for steady state  
114 magnetization. Participants’ head was immobilized with the use of foam pads that applied pressure  
115 onto headphones. A structural T<sub>1</sub>-weighted 3D MP-RAGE sequence (voxel size= 1×1×1.2 mm<sup>3</sup>; matrix  
116 size= 240×256; TR= 2300 ms, TE= 2.91 ms, TI= 900 ms, FoV= 256; 160 slices) was also acquired for all  
117 participants.

118 **Analyses.** Functional volumes from the uncrossed and crossed conditions were pre-processed and  
119 analyzed separately using SPM8 (<http://www.fil.ion.ucl.ac.uk/spm/software/spm8/>; Welcome  
120 Department of Imaging Neuroscience, London), implemented in MATLAB (MathWorks). Pre-

121 processing included slice timing correction of the functional time series (Sladky et al., 2011),  
122 realignment of functional time series, co-registration of functional and anatomical data, a spatial  
123 normalization to an echo planar imaging template conforming to the Montreal Neurological  
124 institute space, and a spatial smoothing (Gaussian kernel, 8mm full-width at half-maximum,  
125 FWHM). Serial autocorrelation, assuming a first-order autoregressive model, was estimated using  
126 the pooled active voxels with a restricted maximum likelihood procedure and the estimates were  
127 used to whiten the data and design matrices.

128         Following pre-processing steps, the analysis of fMRI data, based on a mixed effects model,  
129 was conducted in two serial steps accounting respectively for fixed and random effects. For each  
130 subject, changes in brain regional responses were estimated through a general linear model  
131 including the responses to the 2 experimental conditions (uncrossed, crossed). These regressors  
132 consisted of a boxcar function convolved with the canonical hemodynamic response function.  
133 Movement parameters derived from realignment of the functional volumes (translations in x, y and z  
134 directions and rotations around x, y and z axes) and a constant vector were also included as  
135 covariates of no interest. We used a high-pass filter with a discrete cosine basis function and a cut-  
136 off period of 128s to remove artefactual low-frequency trends.

137         Linear contrasts tested the main effect of each condition ([Uncrossed], [Crossed]), the main  
138 effects of general involvement in a tactile TOJ task ([Uncrossed+Crossed]), the specific effect of the  
139 uncrossed condition ([Uncrossed>Crossed]) and the specific effect of the crossed condition  
140 [Crossed>Uncrossed]. These linear contrasts generated statistical parametric maps [SPM(T)]. The  
141 resulting contrast images were then further spatially smoothed (Gaussian kernel 8 mm FWHM) and  
142 entered in a second-level analysis, corresponding to a random effects model, accounting for inter-  
143 subject variance. One-sample t-tests were run on each group separately. Analyses characterized the  
144 main effect of each condition ([Uncrossed], [Crossed]), the main effect of general TOJ  
145 ([Uncrossed+Crossed]), the specific effects of the uncrossed ([Uncrossed>Crossed]) and the crossed

146 condition [Crossed>Uncrossed]. Two-sample t-tests were then performed to compare these effects  
147 between groups ([Blind vs. Sighted]).

148 **Statistical inferences.** Statistical inferences were performed at a threshold of  $p < 0.05$  after  
149 correction for multiple comparisons (Family Wise Error method) over either the entire brain volume,  
150 or over small spherical volumes (15 mm radius) located in structures of interest. Coordinates of  
151 interest for small volume corrections (SVCs) were selected from the literature examining brain  
152 activations related to the external representation of space in sighted participants.

153 Standard stereotactic coordinates (x,y,z) used for SVC (in MNI space).

154 Frontal locations : Left precentral gyrus (preCG): -46, -10, 40 (Matsumoto et al., 2004) ; -46, 8, 46; 24,  
155 4, 58 (Lloyd et al., 2003); -40, 4, 40 (Takahashi et al., 2013). Dorsolateral prefrontal cortex: -52, 14, 26  
156 (Takahashi et al., 2013). Parietal locations: left precuneus (superior parietal lobule): -8, -56, 58 ; -14, -  
157 66, 52 (Matsumoto et al., 2004), -32, -54, 62 (Takahashi et al., 2013); right precuneus: 24, -44, 72 (  
158 Lloyd et al., 2003) ; right posterior parietal cortex (PPC): 26, -54, 42; 24, -54, 58 (Lloyd et al., 2003);  
159 26, -58, 43 (Azañón et al., 2010) ; 24, -51, 42 (Zaehle et al., 2007); left PPC: -46, -64, 38 (Lloyd et al.,  
160 2003); left medial intraparietal area (MIP): -46, -52, 50 (Lloyd et al., 2003). Superior parietal gyrus: -  
161 26, -72, 32 (Takahashi et al., 2013). Temporal locations: right middle temporal gyrus : 46, -40, 2  
162 (Takahashi et al., 2013).

163 **Psychophysiological interaction.** Psychophysiological interaction (PPI) analyses were computed to  
164 identify any brain regions showing a significant change in the functional connectivity with seed  
165 regions (the left precuneus and the left MIP) that showed a significant activation in the ([CB>SC] x  
166 [crossed > uncrossed]) contrast. In each individual, time-series of activity (first eigenvariate) were  
167 extracted from a 10mm sphere centered on the local maxima detected within 10 mm of the  
168 identified peaks in the second level analysis (SC>CB)x(Crossed>Uncrossed). New linear models were  
169 generated at the individual level, using three regressors. One regressor represented the condition  
170 (Crossed > Uncrossed). The second regressor was the activity extracted in the reference area. The  
171 third regressor represented the interaction of interest between the first (psychological) and the



172 second (physiological) regressors. To build this regressor, the underlying neuronal activity was first  
173 estimated by a parametric empirical Bayes formulation, combined with the psychological factor and  
174 subsequently convolved with the hemodynamic response function (Gitelman et al., 2003). The  
175 design matrix also included movement parameters. A significant PPI indicated a change in the  
176 regression coefficients between any reported brain area and the reference region, related to the  
177 experimental condition (Crossed > Uncrossed). Next, individual summary statistic images obtained  
178 at the first level (fixed-effects) analysis were spatially smoothed (6-mm FWHM Gaussian kernel) and  
179 entered in a second-level (random-effects) analysis using a one-sample t-test contrasting CB>SC  
180 and SC>CB. Statistical inferences were conducted as for the main-effect analysis described above.

## 181 **Results**

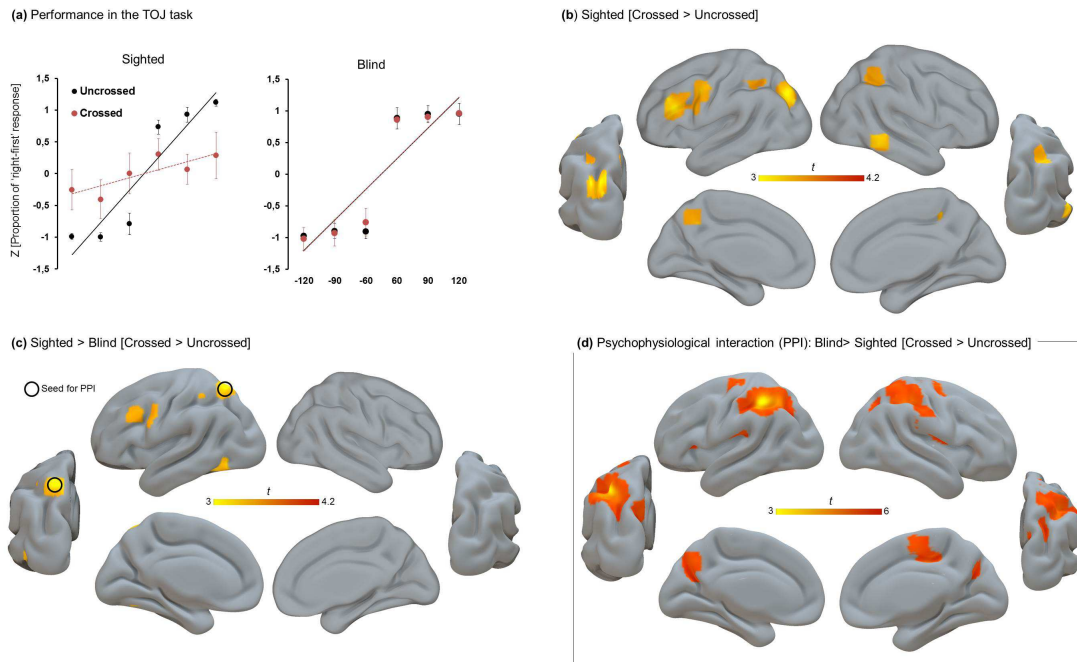
### 182 ***Behavioral data***

183 The slopes of each individual line (calculated from the z-scores of the mean percentages of  
184 “right hand first” responses) were submitted to an ANOVA with posture (uncrossed vs. crossed) as  
185 the within-subject factor and group (SC, CB) as the between-subject variable. Results showed: (1) a  
186 significant effect of posture [ $F(1, 17) = 6.52, p = .02, \eta^2 = .28$ ], the regression line for the uncrossed  
187 posture being steeper ( $M = .95 \pm .01$ ) than the regression line for the crossed posture ( $M = .58 \pm .14$ );  
188 (2) a significant effect of group [ $F(1, 17) = 8.27, p = .01, \eta^2 = .33$ ], the CB ( $M = .97 \pm .11$ ) performing  
189 better (steeper regression) than the SC ( $M = .57 \pm .09$ ); and (3) a significant posture x group  
190 interaction [ $F(1, 17) = 6.75, p = .02, \eta^2 = .28$ ]. To further examine this interaction, paired samples t-  
191 tests compared hand positions in each group separately. In SC, participants’ performance was better  
192 in the uncrossed posture ( $M = .94 \pm .02$ ) than in the crossed posture ( $M = .20 \pm .24$ ), [ $t(10) = -3.04, p =$   
193  $.01$ ]. In deep contrast, the CB group did not show any effect of posture [ $t(7) = 1.05, p = .33$ ], the slope  
194 of the regression lines being similar in the uncrossed ( $M = .96 \pm .004$ ) and crossed postures ( $M = .97 \pm$   
195  $.004$ ). In SC, the Just Noticeable Difference (JND) was equal to 27 ms in the uncrossed position and  
196 125 ms in the crossed posture. In the CB group, the JND was equal to 26 ms in both postures.

### 197 ***fMRI data***

198           We first tested whether our paradigm allowed us to observe the activation of the external  
199 remapping network in SC. Results revealed that the crossed condition, compared to the uncrossed  
200 posture, elicited brain responses in a large fronto-parietal network including the left superior  
201 parietal gyrus, the right posterior parietal cortex (PPC), the left precuneus, the left precentral gyrus,  
202 the left dorso-lateral prefrontal cortex, and the right middle temporal gyrus (see Fig. 1B and Table  
203 2). The same contrast [crossed > uncrossed] performed in the CB group did not reveal any significant  
204 result. When the [crossed > uncrossed] contrast was directly compared between groups [SC vs CB],  
205 SC showed significantly more activity than the CB in the left precuneus, the left MIP, the left dorso-  
206 lateral prefrontal cortex and the right middle temporal gyrus (see Figure 1c and Table 2). CB did not  
207 show more activity than sighted for this contrast in any region.

208           Psychophysiological interaction (PPI) analyses were computed to identify between-group  
209 differences in the functional connectivity maps of the regions involved in the automatic external  
210 remapping of touch identified in the sighted group. For these analyses, the left precuneus (-20, -66,  
211 60 mm) was selected as seed region since it displayed the strongest between-group differences for  
212 the contrast [SC > CB] x [Crossed > Uncrossed] and also because this region was already reported in  
213 the literature as the neural basis of the external remapping of touch (Lloyd et al., 2003; Matsumoto  
214 et al., 2004; Azañón et al., 2010a; Takahashi et al., 2013; Wada et al., 2012). Interestingly, the results  
215 revealed that the seed regions showed stronger connectivity with and extended parietal network in  
216 CB compared to SC for the crossed over uncrossed posture (see Figure 1D).



217  
 218 **Figure 1.** (A) Standardized z-score equivalents of the mean proportions of right-hand responses and  
 219 best-fitting linear regression lines for the uncrossed (black lines) and crossed (red lines) postures for  
 220 sighted and congenitally blind; (B) Results of the whole brain analyses probing brain activity  
 221 obtained from the contrast testing which regions are specifically dedicated to the external  
 222 remapping process in sighted ([Sighted] x [Crossed > Crossed]). There were no activations observed  
 223 for this contrast in the blind group. (C) Regions selectively more active in the sighted group over the  
 224 blind group in the crossed over the uncrossed posture ([Sighted > Blind] x [Crossed > Crossed]). (D)  
 225 Functional connectivity changes. An increase of functional connectivity was observed between the  
 226 left precuneus (seed encircled) and a bilateral fronto-parietal network when congenitally blind  
 227 performed the TOJ task in the crossed over uncrossed posture. Whole brain maps are displayed at  
 228  $p < .001$  uncorrected ( $k > 15$ ) for visualization purpose only (see methods for the assessment of  
 229 statistical significance).

230 **Table 2. Functional results summarizing the main effect of groups for the different contrasts of**  
 231 **interests**

Area	Cluster Size	x	y	z	Z	p
<b>(A) [SC] x [Crossed &gt; Uncrossed]</b>						
L superior parietal gyrus	89	-28	-80	36	3.68	0.004*
R PPC	204	22	-46	46	3.64	0.004*
L precuneus	99	-14	-56	50	3.16	0.017*
L PreCG	142	-40	-2	40	3.41	0.008*
L dorso-lateral prefrontal cortex	91	-60	10	30	3.36	0.01*
R middle temporal gyrus	42	40	-46	-2	3.50	0.006*
<b>(B) [CB] x [Crossed &gt; Uncrossed]</b>						
No Significant Responses						

**(C) [SC > CB] x [Crossed > Uncrossed]**

with inclusive mask (0.001) of [SC] x [Crossed > Uncrossed]

L Precuneus	81	-20	-66	60	3.31	0.01*
L MIP	20	-46	-46	58	3.21	0.01*
L dorso-lateral prefrontal cortex	79	-52	8	38	3.15	0.01*
L precentral gyrus	15	-48	18	36	3.11	0.02*
R MTG	25	40	-44	-4	3.20	0.01*

**(D) [CB > SC] x [Crossed > Uncrossed]**

No Significant Responses

**(E) PPI -20 -66 60 [CB > SC] x [Crossed > Uncrossed]**

with inclusive mask (0.001) of [CB] x [Crossed > Uncrossed]

L MIP	1381	-40	-46	52	4.69	0.03 <sup>#</sup>
R PPC	1348	28	-42	48	4.22	0.001*
R IPS	127	20	-64	36	3.45	0.01*

232

233 Table 1. Brain activations significant ( $p_{corr} < .05$  FWE) after correction over over the whole brain  
 234 volume (<sup>#</sup>) or over small spherical volumes of interest (\*). Cluster size represents the number of  
 235 voxels in specific clusters when displayed at  $p(\text{uncorr}) < .001$ . SC: sighted controls, CB: congenitally  
 236 blind, L: left, R: Right, MIP: medial intraparietal area, MTG: middle temporal gyrus, PPC: posterior  
 237 parietal cortex; IPS: intraparietal sulcus.

238 **Discussion**

239 We assessed the role visual experience plays in shaping the neural correlates of tactile  
 240 localization. For this purpose, SC and CB participants were scanned while performing TOJ  
 241 judgments with the hands uncrossed or crossed over the body midline. At a behavioral level, we  
 242 observed that crossing the hands massively disrupted TOJ performance in SC but not in CB (see  
 243 Figure 1A), replicating previous demonstration by Röder et al. (2004). While exploring the  
 244 neurophysiological underpinning of this effect, we observed that the crossed condition, when  
 245 compared to the uncrossed posture, elicited significantly more activity in the parietal and premotor  
 246 areas in sighted, but not in blind participants. Our findings thus compellingly demonstrated that  
 247 visual experience plays a crucial role in the development and/or engagement of a parieto-frontal  
 248 network involved in this coordinate transformation process.

249 In sighted individuals, vision is a dominant sense for processing space due to the typically  
 250 higher reliability, when compared to other senses, of the signal it provides for such a process. For  
 251 instance, auditory or tactile information are typically remapped toward visual positions if inputs are  
 252 spatially misaligned (Alais and Burr, 2004; Charbonneau et al., 2013); owls reared with prisms

253 deviating their vision show permanent biases in auditory localization (Knudsen and Knudsen, 1989);  
254 and short-term adaptation to spatially conflicting visual and auditory stimuli biases auditory  
255 localization toward the visual source (Recanzone, 1998; Zwiers et al., 2003). Vision can even over-  
256 ride the proprioceptive sensation of a limb in space by displacing the position of a hidden arm  
257 toward a rubber one (Botvinick and Cohen, 1998). Actually, when we hear or feel something  
258 approaching or touching the body, we typically orient our vision toward this event and then use our  
259 motor system to guide appropriate action plans based on a precise location of the target in the  
260 external world (Goodale, 2011). As a result of their lack of visual experience, congenitally blind  
261 people have to rely exclusively on spatial information delivered by the remaining intact senses, such  
262 as hearing and touch. Thus, it seems likely that spatial perception in congenitally blind and in  
263 sighted people develops along different trajectories, and operates in a qualitatively different way in  
264 adulthood. Several studies have indeed pointed toward a reduced sense of external space in early  
265 blind individuals (Andersen et al., 1984; Bigelow, 1987; Dunlea, 1989; Millar, 1994; Ruggiero et al.,  
266 2012).

267         It has been shown that parietal and dorsal premotor regions play a crucial role in co-  
268 registering spatial information collected from various senses and frames of reference into a common  
269 coordinate system for the guidance of both eye and limb movements onto the external world  
270 (Graziano et al., 1994, 1997; Duhamel et al., 1998; Colby and Goldberg, 1999; Lloyd et al., 2003;  
271 Mulette-Gillman et al., 2005; Makin et al., 2007). For instance, it was shown that the position of the  
272 arm is represented in the premotor (Graziano, 1999) and parietal (Graziano, 200) cortex of the  
273 monkey by means of a convergence of visual and proprioceptive cues onto the same neurons. More  
274 particularly, these regions are thought to be part of a network responsible for the remapping of skin-  
275 based touch representations located in somatosensory regions into external spatial coordinates  
276 (Lloyd et al., 2003; Matsumoto et al., 2004; Bolognini and Maravita, 2007; Zhaele et al., 2007;  
277 Azañón et al., 2010a; Longo et al., 2010; Takahashi et al., 2013; Wada et al., 2012). Accordingly,  
278 transiently disrupting the activity of the right posterior parietal cortex with Transcranial Magnetic

279 Stimulation (TMS) selectively impairs the tactile remapping process but does not disrupt  
280 proprioceptive and somatosensory localization processes, highlighting the causal role of this region  
281 in remapping touch into external space (Azañón et al., 2010a).

282         When the hands are crossed, the conflict between external and anatomical representations  
283 of the hands increases the computational demands of the external remapping process which is  
284 typically observed in the “default” uncrossed posture (Melzack and Bromage, 1973; Bromage, 1974).  
285 Crossing the hands therefore triggers enhanced activity in the dorsal parieto-frontal network (see  
286 Figure 1B). In early blind people, the absence of a mandatory external remapping process prevents  
287 the increased recruitment of this neural network while crossing the hands. Therefore, by using  
288 blindness as a model system, we demonstrated that developmental vision plays a causal role in  
289 developing the computational architecture of parietal and dorsal premotor regions for transforming  
290 tactile coordinates from an initial skin-based representation to a representation that is defined by  
291 coordinates in external space.

292         Interestingly, it has recently been suggested that the integration of spatial information from  
293 different reference frames actually depends on the relative weight attributed to the internal and  
294 external coordinates (Azañón et al., 2010a; Badde et al., 2015; Badde and Heed, 2016). While  
295 integration seems mandatory in SC (Yamamoto and Kitazawa, 2001; Shore et al., 2002, Azañón et  
296 al., 2010b) the relative weight attributed to each coordinate system seems to be more dependent on  
297 tasks demands and instructions in CB (Heed and Röder, 2014; Heed et al., 2015; Crollen et al., 2017).  
298 Further studies should examine whether the external remapping network could therefore be active  
299 in CB while performing a task emphasizing external instructions. It is indeed possible that the  
300 external coordinate system is less automatically activated in CB than in SC but this does not mean  
301 that this system is not readily accessible when the task requires it (as, for example, when people  
302 perform an action directed toward the external world: Fiehler et al., 2009; Lingnau et al., 2014).

303         A recent study in the sighted demonstrated that the crossed-arms posture elicited stronger  
304 functional connectivity between the left IPS on the one hand and the right frontal gyrus and the left

305 PPC on the other hand (Ora et al., 2016). By performing task-dependent functional connectivity  
306 analyses (Psychophysiological interactions), we demonstrate that blind individuals rely on enhanced  
307 integration between dorsal regions (Heine et al., 2015) while experiencing a conflict between body-  
308 centered and world-centered coordinates (see Figure 1D). This raises the intriguing possibility that  
309 changes in the connectivity pattern of the parietal cortex gates the activation, or not, of the external  
310 remapping process in congenitally blind people depending on task demands. Enhanced parieto-  
311 frontal connectivity in the crossed posture in the blind may therefore prevent the automatic  
312 remapping process from occurring in a task that does not necessitate such a computation (the TOJ  
313 task can be resolved by using pure skin-based coordinates). This could potentially explain the  
314 enhanced performance of the blind population in the crossed condition of the TOJ task (see Figure  
315 1A).

316 In conclusion, we demonstrate that early visual deprivation alters the development of the  
317 brain network involved in the automatic multisensory integration of touch and proprioception into a  
318 common, external, spatial frame of reference. Moreover, the enhanced connectivity between dorsal  
319 regions in CB may provide a mechanistic framework to understand how blind people differently  
320 weight specific spatial coordinate systems depending on the task at play (Badde et al., 2015; Badde  
321 and Heed, 2016). These results have far-reaching implications for our understanding of how visual  
322 experience calibrates the development of brain networks dedicated to the spatial processing of  
323 touch.

324

325 **Author contributions:** VC and OC designed research; VC, LL, and AB performed research; VC, OC,  
326 and MR analyzed data; VC and OC wrote the paper; FL provided laboratory resources for the  
327 optimal recruitment and testing of participants.

328

329

330

331 **References**

- 332 Alais D, Burr D (2004) The ventriloquist effect results from near-optimal bimodal integration.  
333 *Curr Biol* 14(3): 257–262.
- 334 Andersen ES, Dunlea A, Kekelis LS (1984) Blind children’s language: resolving some  
335 differences. *J Child Lang* 11(3): 645–664.
- 336 Azañón E, Soto-Faraco S (2008) Changing reference frames during the encoding of tactile  
337 events. *Curr Biol*. 18 (14): 1044–1049.
- 338 Azañón E, Camacho K, Soto-Faraco S (2010) Tactile remapping beyond space. *Eur J*  
339 *Neurosci* 31(10): 1858–1867 (2010).
- 340 Azañón E, Longo MR, Soto-Faraco S, Haggard P (2010) The posterior parietal cortex remaps  
341 touch into external space. *Curr Biol*. 20(14): 1304–1309.
- 342 Azañón E, Stenner MP, Cardini F, Haggard P (2015) Dynamic tuning of tactile localization to  
343 body posture. *Curr Biol* 25(4): 512–517.
- 344 Badde S, Röder B, Heed T (2015) Flexibly weighted integration of tactile reference frames.  
345 *Neuropsychologia* 70: 367–374.
- 346 Badde S, Heed T (2016) Towards explaining spatial touch perception: weighted integration  
347 of multiple location codes. *Cogn Neuropsychol* 33(1-2): 26–47.
- 348 Bigelow A (1987) Early words of blind children. *J Child Lang*. 14: 47–56.
- 349 Bolognini N, Maravita A (2007) Proprioceptive alignment of visual and somatosensory maps  
350 in the posterior parietal cortex. *Curr Biol* 17(21): 1890–1895.
- 351 Botvinick M, Cohen J (1998) Rubber hands “feel” touch that eyes see. *Nature* 391(6669): 756.
- 352 Bromage PR (1974) Phantom limbs and the body schema. *Canadian Anaesthetists' Society*  
353 *journal* 21(3): 267.
- 354 Charbonneau G, Véronneau M, Boudrias-Fournier C, Lepore F, Collignon O (2013) The  
355 ventriloquist in periphery : impact of eccentricity-related reliability on audio-visual localization. *J Vis*  
356 13(12): 20.



- 357 Colby CL, Goldberg ME (1999) Space and attention in parietal cortex. *Annu Rev Neurosci* 22:  
358 319–349.
- 359 Crollen V, Albouy G, Lepore F, Collignon O (2017) How visual experience impacts the internal  
360 and external spatial mapping of sensorimotor functions. *Sci Rep* 7(1): 1022.
- 361 Duhamel JR, Colby CL, Goldberg ME (1998) Ventral intraparietal area of the macaque:  
362 congruent visual and somatic response properties. *J Neurophysiol* 79: 126–136.
- 363 Dunlea A (1989) *Vision and the Emergence of Meaning. Blind and Sighted Children’s Early*  
364 *Language*. Cambridge University Press, Cambridge, UK.
- 365 Fiehler K, Burke M, Bien S, Röder B, Rösler F (2009) The human dorsal action control system  
366 develops in the absence of vision. *Cereb Cortex* 19(1): 1–12.
- 367 Gitelman DR, Penny WD, Ashburner J, Friston KJ (2003) Modeling regional and  
368 psychophysiologic interactions in fMRI: the importance of hemodynamic deconvolution.  
369 *NeuroImage* 19(1): 200–207
- 370 Goodale MA (2011) Transforming vision into action. *Vision Res* 51(13): 1567–1587.
- 371 Graziano MSA, Yap GS, Gross CG (1994) Coding of visual space by premotor neurons.  
372 *Science* 266(5187): 1054–1057.
- 373 Graziano MSA, Hu XT, Gross CG (1997) Visuo-spatial properties of ventral premotor cortex. *J*  
374 *Neurophysiol* 77: 2268–2292.
- 375 Graziano MSA (1999) Where is my arm? The relative role of vision and proprioception in the  
376 neuronal representation of limb position. [Proc Natl Acad Sci U S A](#) 96(18): 10418–10421.
- 377 Graziano MSA, Cooke DF, Taylor CSR (2000) Coding the Location of the Arm by Sight.  
378 *Science* 290(5497): 1782–1786.
- 379 Heed T, Azañón E (2014) Using time to investigate space: a review of tactile temporal order  
380 judgments as a window onto spatial processing in touch. *Front Psychol* 5: 76.
- 381 Heed T, Röder B (2014) Motor coordination uses external spatial coordinates independent of  
382 developmental vision. *Cognition* 132: 1–15.

- 383 Heed T, Möller J, Röder B (2015) Movement induces the use of external spatial coordinates  
384 for tactile localization in congenitally blind humans. *Multisens Res* 28: 173–194.
- 385 Heine L, Bahri MA, Cavaliere C, Soddu A, Laureys S, Ptito M, Kupers R (2015) [Prevalence of](#)  
386 [increases in functional connectivity in visual, somatosensory and language areas in congenital](#)  
387 [blindness](#). *Front Neuroanat* 9: 86.
- 388 Knudsen EI, Knudsen PE (1989) Vision calibrates sound localization in developing barn owls.  
389 *J Neurosci* 9(9): 3306–3313.
- 390 Lingnau A, Strnad L, He C, Fabbri S, Han Z, Bi Y, Caramazza A (2014). Cross-modal plasticity  
391 preserves functional specialization in posterior parietal cortex. *Cereb Cortex* 24(2): 541–549 (2014).
- 392 Lloyd DM, Shore DI, Spence C, Calvert GA (2003) Multisensory representation of limb  
393 position in human premotor cortex. *Nat Neurosci* 6(12): 17–18.
- 394 Longo MR, Azañón E, Haggard P (2010). More than skin deep: Body representation beyond  
395 primary somatosensory cortex. *Neuropsychologia* 48(3): 655–668.
- 396 Makin TR, Holmes NP, Zohary E (2007) Is that near my hand? Multisensory representation of  
397 peripersonal space in human intraparietal sulcus. *J Neurosci* 27(4): 731–740.
- 398 Matsumoto E, Misaki M, Miyauchi S (2004) Neural mechanisms of spatial stimulus-response  
399 compatibility: the effect of crossed-hand position. *Exp Brain Res* 158: 9–17.
- 400 Melzack R, Bromage PR (1973) Experimental phantom limbs. *Experimental Neurology* 39(2):  
401 261–269.
- 402 Millar S (1994). *Understanding and Representing Space. Theory and Evidence From Studies*  
403 *With Blind and Sighted Children*. Oxford: Clarendon Press.
- 404 Mullette-Gillman OA, Cohen YE, Groh JM (2005) Eye-Centered, Head-Centered, and  
405 Complex Coding of Visual and Auditory Targets in the Intraparietal Sulcus. *J Neurophysiol* 94(4):  
406 2331–2352.
- 407 Ora H, Wada M, Salat D, Kansaku K (2016) Arm crossing updates brain functional  
408 connectivity of the left posterior parietal cortex. *Sci Rep* 6: 28105.

409 Recanzone GH (1998) Rapidly induced auditory plasticity: the ventriloquism aftereffect. Proc  
410 Natl Acad Sci U S A 95(3): 869–875.

411 Röder B, Rösler F, Spence C (2004) Early vision impairs tactile perception in the blind. Curr  
412 Biol 14: 121–124.

413 Ruggiero G, Ruotolo F, Iachini T (2012) Egocentric/allocentric and coordinate/categorical  
414 haptic encoding in blind people. Cogn Process Suppl 1: S313-7.

415 Shore DI, Spry E, Spence C (2002) Confusing the mind by crossing the hands. Brain Res Cogn  
416 Brain Res 14: 153–163.

417 Sladky R, Friston KJ, Tröstl J, Cunnington R, Moser E, Windischberger C (2011) Slice-timing  
418 effects and their correction in functional MRI. NeuroImage 58(2): 588-594.

419 Takahashi T, Kansaku K, Wada M, Shibuya S, Kitazawa S (2013) Neural correlates of tactile  
420 temporal-order judgment in humans: an fMRI study. Cereb Cortex 23: 1952–1964.

421 Yamamoto S, Kitazawa S (2001) Reversal of subjective temporal order due to arm crossing.  
422 Nat Neurosci 4: 759–765.

423 Wada M, Takano K, Ikegami S, Ora H, Spence C, Kansaku K (2012) Spatio-temporal updating  
424 in the left-posterior parietal cortex. Plos One 7(6): e39800.

425 Zaehle T, Jordan K, Wüstenberg T, Baudewig J, Dechent P, Mast FW (2007) The neural basis  
426 of the egocentric and allocentric spatial frame of reference. Brain Res 1137(1): 92–103.

427 Zwiers MP, Van Opstal AJ, Paige GD (2003) Plasticity in human sound localization induced  
428 by compressed spatial vision. Nat Neurosci 6(2): 175–181.

429

430

431

432

433

434

435 **Figure legend**

436 **Figure 1.** (A) Standardized z-score equivalents of the mean proportions of right-hand  
437 responses and best-fitting linear regression lines for the uncrossed (black lines) and crossed (red  
438 lines) postures for sighted and congenitally blind; (B) Results of the whole brain analyses probing  
439 brain activity obtained from the contrast testing which regions are specifically dedicated to the  
440 external remapping process in sighted ([Sighted] x [Crossed > Crossed]). There were no activations  
441 observed for this contrast in the blind group. (C) Regions selectively more active in the sighted group  
442 over the blind group in the crossed over the uncrossed posture ([Sighted > Blind] x [Crossed >  
443 Crossed]). (D) Functional connectivity changes. An increase of functional connectivity was observed  
444 between the left precuneus (seed encircled) and a bilateral fronto-parietal network when  
445 congenitally blind performed the TOJ task in the crossed over uncrossed posture. Whole brain maps  
446 are displayed at  $p < .001$  uncorrected ( $k > 15$ ) for visualization purpose only (see methods for the  
447 assessment of statistical significance).

448

449

450

451

452

453

454

455

456